

# Dynamics of two colliding Bose-Einstein condensates in an elongated magneto-static trap

M. Modugno<sup>1</sup>, F. Dalfovo<sup>2</sup>, C. Fort<sup>1</sup>, P. Maddaloni<sup>1\*</sup>, and F. Minardi<sup>1</sup>

<sup>1</sup> *INFM – L.E.N.S. – Dipartimento di Fisica, Università di Firenze  
L.go E. Fermi 2, I-50125 Firenze, Italy*

<sup>2</sup> *Dipartimento di Matematica e Fisica, Università Cattolica,  
and Istituto Nazionale per la Fisica della Materia, Gruppo Collegato di Brescia,  
Via Musei 41, I-25121 Brescia, Italy*

(October 22, 2018)

We study the dynamics of two interacting Bose-Einstein condensates, by numerically solving two coupled Gross-Pitaevskii equations at zero temperature. We consider the case of a sudden transfer of atoms between two trapped states with different magnetic moments: the two condensates are initially created with the same density profile, but are trapped into different magnetic potentials, whose minima are vertically displaced by a distance much larger than the initial size of both condensates. Then the two condensates begin to perform collective oscillations, undergoing a complex evolution, characterized by collisions between the two condensates. We investigate the effects of their mutual interaction on the center-of-mass oscillations and on the time evolution of the aspect ratios. Our theoretical analysis provides a useful insight into the recent experimental observations by Maddaloni *et al.*, cond-mat/0003402.

03.75.Fi, 05.30.Jp, 34.20.Cf

## I. INTRODUCTION

Several papers have been recently devoted to the study of multiple-species interacting Bose-Einstein condensates (BEC) [1–9]. The first experiments involving the interaction between multiple condensates have been performed at JILA, with two condensates in the hyperfine levels  $|F = 2, m_f = 2\rangle$  and  $|1, -1\rangle$  of  $^{87}\text{Rb}$  confined in a Ioffe-type trap [2]. Other experiments have been performed with the states  $|2, 1\rangle$  and  $|1, -1\rangle$  in a TOP trap, in a situation of nearly complete spatial overlap of the two condensates. In fact they have almost the same magnetic moment and therefore experience two (slightly displaced) trapping potentials with the same frequencies [3–5]. The resulting dynamics reveals a complex structure and it is characterized by a strong damping of the relative motion of the two condensates [3]. These results have been analyzed in [8], by identifying two dynamical regimes: (i) a periodic motion with a slow frequency (with respect to the trap frequency), for small displacement between the traps; (ii) a strong non-linear mixing which leads to a damping of the relative motion, for larger displacements (but still smaller than the size of the initial condensate). By comparing the numerical solution of the Gross-Pitaevskii equation with the JILA experi-

ment [3], the authors of Ref. [8] find a fair agreement, although small oscillations remain undamped for longer times compared to the experimental observation [8,9].

A mixture of  $^{87}\text{Rb}$  condensates in different  $m_f$  states in a TOP trap has been experimentally investigated also by another group [6], but no effects of the mutual interaction have been observed.

Recently we have reported some experiments performed at LENS with two interacting condensates [1], which reveal several new features with respect to those analyzed in Refs. [3,8]. In fact, we have considered a sudden transfer of atoms between the states  $|2, 2\rangle$  and  $|2, 1\rangle$  of  $^{87}\text{Rb}$ , having different magnetic moments. The  $|2, 1\rangle$ , which is created with the same density distribution and at the same position of the  $|2, 2\rangle$  condensate, feels a magnetic potential whose minimum is displaced along the vertical  $y$  axis by a distance much larger than the initial size of the condensate. Therefore, its dynamics is characterized by large center-of-mass oscillations. The two condensates periodically collide and these collisions have significant observable effects. Among them: i) the shape oscillations of  $|2, 2\rangle$  condensate, triggered by the sudden transfer to the  $|2, 1\rangle$  state, are significantly enhanced; ii) the center-of-mass oscillation frequency of the  $|2, 1\rangle$  condensate is shifted upwards.

By means of preliminary numerical simulations, we have already shown that the basic features of these experimental observations can be explained within the Gross-Pitaevskii (GP) theory [1]. In this paper we better analyse the theoretical scheme and describe in more detail the numerical procedures and the approximations made.

The paper is organized as follows: in Section II, we introduce the two coupled GP equations for the dynamics of the condensates and discuss the approximations used to solve them. In Section III we show the results for the center-of-mass motion, stressing the effect of mutual interactions in the oscillation frequency. In Section IV we discuss the collective modes of each condensate and the time evolution of the aspect ratios. In Section V we simulate the expansion of the two condensates after switching-off the trapping potential. In this way, we can compare our theoretical results with the experimental data [1] for the center-of-mass motion and the aspect ratios.

## II. GROSS-PITAEVSKII THEORY FOR TWO COUPLED CONDENSATES

At very low temperatures, when there is no thermal cloud, the evolution of the two interacting Bose-Einstein condensates can be described by two coupled Gross-Pitaevskii (GP) equations ( $i = 1, 2$ ):

$$i\hbar \frac{\partial \Psi_i}{\partial t} = \left[ -\frac{\hbar^2 \nabla^2}{2m} + V_i + \sum_{j=1,2} \frac{4\pi\hbar^2 a_{ij}}{m} |\Psi_j|^2 \right] \Psi_i. \quad (1)$$

Here,  $\Psi_1$  and  $\Psi_2$  are the order parameters of the  $|2, 1\rangle$  and  $|2, 2\rangle$  condensates of  $^{87}\text{Rb}$  (hereafter called  $|1\rangle$  and  $|2\rangle$ ). By solving Eq. (1) we want to simulate the situation in which a certain amount of atoms are suddenly transferred from the condensate  $|2\rangle$ , initially in its ground state in the trap, to the condensate  $|1\rangle$ . Due to the different magnetic moment, the condensate  $|1\rangle$  experiences a trapping potential having the axial and radial frequencies lowered by a factor  $\sqrt{2}$  and the minimum shifted radially by a constant value. Thus, the trapping potential  $V_i$  are different and can be written as

$$V_1(x, y, z) = \frac{m}{2} \omega_{\perp 1}^2 [x^2 + (y + y_0)^2 + \lambda^2 z^2] \quad (2)$$

$$V_2(x, y, z) = \frac{m}{2} \omega_{\perp 2}^2 [x^2 + y^2 + \lambda^2 z^2]. \quad (3)$$

From now on we use the same parameters as in the experiments of Ref. [1], that is: scattering lengths  $a_{22} = a_{12} \simeq 98a_0$  and  $a_{11} \simeq 94.8a_0$ , trapping frequencies  $\omega_{\perp 2} = 2\pi \times 164.5$  Hz,  $\omega_{\perp 1} = \omega_{\perp 2}/\sqrt{2} = 2\pi \times 116.3$  Hz, and displacement  $y_0 = g/\omega_{\perp 2}^2 = 9.2\mu\text{m}$ . The two condensates have the same asymmetry parameter  $\lambda \equiv \omega_z/\omega_{\perp} \simeq 0.0766$ . For the total number of atoms we use  $N = N_1 + N_2 = 1.5 \times 10^5$  with  $N_1 = 0.13N$ .

In order to numerically solve the GP equations (1) one should map the two order parameters  $\Psi_i$  on a fully three-dimensional grid of points. This should be large enough to describe the oscillations of each condensate in the trap (center-of-mass motion plus internal excitations) as well as their expansion when the trap is switched off. This approach is computationally heavy. We prefer, at this stage, to solve the GP equations (1) within different approximate schemes, depending on the type of process we want to describe. We distinguish the following three cases.

Case A: dynamics of a condensate in the trap ignoring its interaction with the other. In this case, the center-of-mass (CM) motion is trivial: the CM of the condensate  $|2\rangle$  remains at rest, while the one of  $|1\rangle$  oscillates freely around  $y_0$  at the frequency  $\omega_{\perp 1}$ . The internal motion of each condensate originates from the fact that its starting configuration, after transferring atoms from  $|2\rangle$  to  $|1\rangle$ , is not the ground state configuration. In particular, the state  $|2\rangle$  feels the same trap but has less atoms: its starting shape is wider than the equilibrium one. Its internal motion can be predicted by exactly solving the corresponding GP equation, without coupling with  $|1\rangle$ ,

i.e., with  $a_{12} = 0$ . In this case, the equation has axial symmetry and we can use the numerical code developed by two of us in Ref. [10].

Case B: effects of the mutual interaction in the radial motion. In order to point out the basic effects of the interaction occurring between the two condensates when they collide, one can decouple the slow axial motion from the GP equation. In this way, the simulation is reduced to a two-dimensional problem in the  $xy$ -plane, which is easier to perform. We solve the coupled GP equations by using the Split-Step Fourier method [11], with a Fast Fourier Transform algorithm [12], by using cylindrical coordinates and dimensionless variables, as explained in the Appendix. We will justify the decoupling of the axial motion later, when discussing the low energy collective modes of these condensate.

Case C: dynamics of the free expansion. In the experiments, the CM positions and the aspect ratios of the condensates are measured after few milliseconds of expansion, with the trap switched off. We simulate the expansion, starting from the configuration obtained in case A or B at a given time. The CM of the two condensates simply undergo a free fall under gravity. The shape of each condensate changes during the expansion. We simulate the expansion of the condensate  $|2\rangle$  by using a scaling law valid in the Thomas-Fermi (large  $N$ ) limit [13,14]. We instead ignore the mutual interaction of the condensates in this process; even if they overlap after some time (see Section V), their density is much lower than the initial one, due to the fast radial expansion, and hence the mean-field interaction is also much weaker.

## III. CENTER-OF-MASS MOTION IN THE TRAP

We start from an initial configuration corresponding to the lowest stationary solution of Eq. (1), with  $N$  atoms in the  $|2\rangle$  condensate. This can be obtained by iterating in imaginary time, starting from a trial wave function, as done in [15]. Then, at an arbitrary time  $t = 0$ , one builds two condensates  $|1\rangle$  and  $|2\rangle$ , with the same density profile of the starting one, but with different number of atoms,  $N_1$  and  $N_2$ .

If they do not interact ( $a_{12} = 0$ ), the CM of condensate  $|2\rangle$  remains at rest, while the one of the condensate  $|1\rangle$  starts oscillating around its equilibrium position  $y = -y_0$  with frequency  $\omega_{\perp 1}$ , as shown in Fig. 1a.

In order to include the effects of the mutual interaction, we make a two-dimensional simulation as explained in case B of the previous Section, by ignoring the axial motion and solving the two coupled GP equations in the  $xy$ -plane. Thus, the initial condensate is an infinite cylinder along  $z$  while the normalization of the two-dimensional order parameter in the  $xy$ -plane is chosen in such a way to preserve the profile in the radial direction, when passing from 3 to 2 dimensions, as explained in the Appendix. The results are shown in Fig. 1b. One

sees that now both condensates move. The motion of the condensate  $|2\rangle$  originates from the mutual repulsion with the condensate  $|1\rangle$ , which acts both at the beginning, when  $|1\rangle$  is formed and starts moving away from  $|2\rangle$ , and when they periodically collide. The motion of  $|1\rangle$  is still dominated by large oscillations around  $-y_0$ , but their frequency  $\omega_1$  turns out to be larger than the non-interacting frequency  $\omega_{\perp 1}$  by about 5.4%. Furthermore, the oscillations appear to be damped. We notice that, though the minimum separation between the two center-of-mass positions slowly grows in time, it remains always smaller than the sum of the two condensate radii, at least in time interval here considered, thus ensuring that the two condensates indeed collide.

The shift in frequency of the CM oscillations is one of the clear signatures of the mutual interaction. It originates from the fact that the condensate  $|1\rangle$  moves in an effective trap which is anharmonic. In fact, the presence of the condensate  $|2\rangle$  at one side of the harmonic potential in which  $|1\rangle$  moves, provide an extra repulsion with a consequent up-shift of frequency. This shift only occurs if the two condensates overlap periodically. Since it comes from the cross mean-field term in the GP equation, it depends significantly on  $N_2$ .

Indeed, as a first approach we can consider the 1D problem of one single classical particle moving in the effective potential  $V_e(y)$  given by the harmonic oscillator plus the repulsion of the  $|2\rangle$  atoms:

$$V_e(y) = \frac{m}{2}\omega_{\perp 1}^2 y^2 + g_{21}n_0 \max\left\{0, 1 - \frac{(y + y_0)^2}{R_{\perp 2}^2}\right\} \quad (4)$$

where  $g_{21} = 4\pi\hbar^2 a_{21}/m$ , while  $R_{\perp 2}$  and  $n_0$  are the radius and the central density of the  $|2\rangle$  condensate in the Thomas-Fermi (large  $N$ ) limit, respectively [14]. To obtain the oscillation period, we carry out two integrals

$$T = \sqrt{2m} \int_{-y_0}^{-y_0+R_{\perp 2}} dy \left[ V_e(-y_0) - \frac{m}{2}\omega_{\perp 1}^2 y^2 + g_{21}n_0 \left(1 - \frac{(y + y_0)^2}{R_{\perp 2}^2}\right) \right]^{-1/2} + \sqrt{2m} \int_{-y_0+R_{\perp 2}}^{y_i} dy \left( V_e(-y_0) - \frac{m}{2}\omega_{\perp 1}^2 y^2 \right)^{-1/2} \quad (5)$$

where  $y_i$  indicates the classical inversion point, equal to  $\sqrt{y_0^2 + 2R_{\perp 2}^2}$ . We find

$$T = \frac{2}{\omega_{\perp 1}} \left[ \frac{\pi}{2} + \arcsin\left(\frac{1 - R_{\perp 2}/y_0}{\sqrt{1 + 2R_{\perp 2}^2/y_0^2}}\right) + \operatorname{arcosh}\left(1 + \frac{R_{\perp 2}}{y_0}\right) \right]. \quad (6)$$

The period depends on the number of atoms only through the radius  $R_{\perp 2}$  that scales as  $N_2^{1/5}$ . In Fig. 2 we see that the frequency shift predicted by Eq. (6) is nicely close to the GP results.

One can better visualize the effects of the interactions in the collisions by plotting the various energy terms contributing to the total energy of the system, as in Fig. 3. We checked that the total energy is accurately conserved during the simulation. The energies of each condensate (kinetic, mean-field, trapping) vary with time in a characteristic way: they change only when the condensates collide. This happens about every 8 ms. During the short collision time, when they partially overlap, the mutual interaction energy, i.e., the term containing the scattering length  $a_{12}$ , is significantly non-zero. In the upper part of the same figure we redraw the CM position of the condensate  $|2\rangle$ , with a vertical scale larger than in Fig. 1. One notices that the slope of these oscillations changes whenever the two condensates collide, the precise change (sign and amplitude) depending on the phase of the oscillation when each collision occurs.

The behavior of the energy *vs.* time is strictly related to the damping of the CM oscillations of condensate  $|1\rangle$ , shown in Fig. 1b. First, we remind that in the GP theory the damping is not due to dissipative processes, since the total energy is conserved. What happens, instead, is that the kinetic energy initially associated with the CM motion is eventually shared among many degrees of freedom. This redistribution of energy is caused by the periodic collisions. One of these degrees of freedom is the CM motion of the condensate  $|2\rangle$ . But the internal excited states of each condensate are also expected to play an important role, as discussed in the next section.

#### IV. CONDENSATE DEFORMATIONS AND ASPECT RATIOS IN THE TRAP

Let us consider the internal motion of the condensate  $|2\rangle$ . Just after the transfer of  $N_1$  atoms into  $|1\rangle$ , its density distribution has the same profile as the ground state of  $N$  atoms, but with 13% of atoms missing. Thus, it starts oscillating around the new equilibrium configuration, the confining potential being unchanged. This situation is very similar to that studied in Ref. [16], where similar oscillations were produced by a sudden change of scattering length.

If one ignores the interaction with the condensate  $|1\rangle$ , the motion of the condensate  $|2\rangle$  can be predicted by solving the GP equation (1) with  $i = 2$  and  $a_{12} = 0$ . This corresponds to case A in Section II. In Fig. 4, we show the resulting aspect ratio,  $[\langle y^2 \rangle / \langle z^2 \rangle]^{1/2}$  (solid line). The curve is clearly a superpositions of two, fast and slow, modes.

To understand which excited states participate in the curve in Fig. 4, we notices that, since the new equilibrium state is not far from the starting configuration, the amplitude of the induced oscillations is relatively small. Therefore, only the lowest energy modes are excited and, among them, the ones with no angular momentum. For an elliptic trap, where only the  $z$ -component of the an-

gular momentum is conserved, two  $m = 0$  states are expected to be excited. The one with lowest frequency corresponds to in-phase oscillations of the width along  $x$  and  $y$  and out-of-phase along  $z$ . The one with highest frequency is an in-phase compressional mode along all directions (breathing mode). In the Thomas-Fermi (TF), large  $N$ , regime and in the linear limit (small amplitude), their frequency is [17]

$$\omega_{\mp} = \sqrt{q_{\mp}} \omega_{\perp 2} \quad (7)$$

with

$$q_{\mp} = 2 + (3/2)\lambda^2 \mp (1/2)\sqrt{9\lambda^4 - 16\lambda^2 + 16}. \quad (8)$$

When the condensate is also strongly elongated ( $\lambda \ll 1$ ) the two frequencies become

$$\omega_{+} \simeq 2 \omega_{\perp 2}; \quad \omega_{-} \simeq \sqrt{\frac{5}{2}} \lambda \omega_{\perp 2}. \quad (9)$$

In this limit the two frequencies are quite different, and the axial and radial collective excitations are almost decoupled. The radial width is characterized by small oscillations of frequency  $\omega_{-}$  superimposed to a wider oscillation of frequency  $\omega_{+}$ , and vice-versa for the axial width [18]. Using the parameters for the condensate  $|2\rangle$  in Eqs. (7)-(8), one finds values which differ less than 0.04% from their asymptotic  $\lambda \rightarrow 0$  values in Eq. (9).

The TF approximation corresponds to neglecting the laplacian of the density (i.e., the quantum pressure) in the GP equation. In this case, the density profile of the condensate in each direction is an inverted parabola which vanishes at the classical turning point. In the radial and axial directions, these points,  $R_{\perp}$  and  $Z$ , are given by the condition  $\mu = m\omega_{\perp 2}^2 R_{\perp}^2/2 = m\omega_{z 2}^2 Z^2/2$ , where  $\mu$  is the chemical potential fixed by the normalization of the order parameter to  $N_2$ . A nice feature of the TF regime is that both the free expansion and the lowest collective modes exhibit an exact scaling behavior: the parabolic shape is preserved and the widths  $R_{\perp}$  and  $Z$  scale as  $R_{\perp}(t) = R_{\perp}(0)b_{\perp}(t)$  and  $Z(t) = Z(0)b_z(t)$ . The GP equation for the condensate  $|2\rangle$  then transforms into two coupled equations for the scaling parameters  $b_{\perp}(t)$  and  $b_z(t)$ :

$$\ddot{b}_{\perp} + \omega_{\perp}^2 b_{\perp} - \frac{\omega_{\perp}^2}{b_{\perp}^3 b_z} = 0 \quad (10)$$

$$\ddot{b}_z + \omega_z^2 b_z - \frac{\omega_z^2}{b_{\perp}^2 b_z^2} = 0. \quad (11)$$

The numerical solution of these differential equations is straightforward. The result for the evolution of the aspect ratio of condensate  $|2\rangle$ ,  $R_{\perp}/Z$ , is shown as a dashed line in Fig. 4 and compared with the one obtained with the exact solution of the GP equation (solid line) for the same condensate,  $[\langle y^2 \rangle / \langle z^2 \rangle]^{1/2}$ . The shape of the two curves is very similar as a consequence of the fact that

the parameter  $Na/a_{ho}$ , with  $a_{ho} = [\hbar/(m\omega_{ho})]^{1/2}$ , is indeed much greater than 1, as required to ensure the validity of the TF approximation. They differ only for a small vertical shift due to the different definitions of the aspect ratio; this shift would vanish only in the  $N \rightarrow \infty$  limit [19].

The aspect ratio in Fig. 4 ignores the mutual interaction between the two condensates in the periodic collisions. Since this interaction breaks the axial symmetry in the motion of  $|2\rangle$ , one should solve the coupled GP equation in full three-dimensions. Here we proceed differently. We observe that the axial motion is much slower than both the time interval between two collisions and the duration of a single collision. We thus assume that the axial motion does not respond significantly to the mutual interaction in the time scale here considered. Vice-versa, the collisions are expected to significantly affect the radial motion. We treat the radial motion by solving numerically the GP equation in the  $xy$ -plane, including the mutual interaction (case B of Section II). In this case, the collisions with the  $|1\rangle$  condensate make the radial motion of  $|2\rangle$  rather complex. Assuming the axial width to be the same as without collisions, and using the radial width obtained by the 2D integration of the coupled GP equations, one can calculate the new aspect ratio. This is given in Fig. 5. One notices that, similarly to what we have found for the center-of-mass motion in Fig. 1b, the shape of the oscillation change at each collision, every 8 ms. The evolution of the aspect ratio has a complex structure and it is not a simple superposition of the two oscillations  $\omega_{-}$  and  $\omega_{+}$  of the non-interacting case. The overall amplitude is enhanced. This reflects the fact that the energy of the CM oscillation of  $|1\rangle$  is transferred, not only to the CM motion of  $|2\rangle$ , but also to the internal degrees of freedom. This again, may explain part of the damping of the CM oscillations of  $|1\rangle$  in Fig. 1b.

Looking at Fig. 5, one sees also that the interaction between the two condensates produces an initial delay for the onset of collective excitations, compared to the non-interacting case. This originates from the fact that the two condensates are initially created with the same density profile, and the scattering lengths  $a_{22}$  and  $a_{12}$  have the same value. Therefore the  $|2\rangle$  condensate “realizes” to be out-of-equilibrium only when the other condensate has moved away, i.e. after a time of the order of  $1 \div 2$  ms. The same effect can be seen in Fig. 3 for the center-of-mass motion.

## V. FREE EXPANSION AND COMPARISON WITH EXPERIMENTS

In the experiments of Ref. [1] the center-of-mass motion and the aspect ratios are measured after releasing the trap and letting the condensate expand under the effect of gravity only.

In order to compare our theoretical predictions with the experimental data we have to include the effects of the expansion. For the center-of-mass motion this is trivial. One has only to take care of the fact that the switch-off of the trapping potential is not instantaneous and can produce a magnetic gradient which affects the initial velocity of the two condensates. The two velocities have been measured experimentally, giving  $v_{1y} = 0.7 \pm 0.1$  cm/s and  $v_{2y} = 1.4 \pm 0.1$  cm/s. Due to this difference, the two condensates fall at different speed and they eventually overlap for some time during the expansion. As already said in Section II (case C), we ignore the mutual mean-field interaction during this process. If the overlap does not occur too early, the condensates have enough time to expand fast in the radial direction, the one of the stronger initial confinement, and their density drops quickly, so that the cross mean-field energy becomes negligible.

Our results for the CM position of the two condensates are shown in Fig. 6. In the upper part (a), we compare theory and experiment in a simple case, in which all the atoms are initially transferred into the condensate  $|1\rangle$ , which then oscillates alone in its new trap. The oscillation is undamped and its frequency is simply the trapping frequency  $\omega_{\perp 1} = 2\pi \times 116.3$  Hz. This picture, in which the mean-field interactions does not enter at all, has been used to fix the small delay caused by the non instantaneous switch-off of the trapping potential. This has been done by introducing the delay as a fitting parameter in the theoretical curve. Its value is  $\simeq 0.6$  ms.

In the lower part of Figs. 6, we compare theory and experiment for the case of the two colliding condensates. The CM dynamics of the two condensates in the trap has been discussed in Section III. Starting from each point in Fig. 1b, we have then added the effect of the fall in the gravity field. At the time of the observation (after 29.3 ms), the condensate  $|1\rangle$  is almost always above the condensate  $|2\rangle$ , which means that they crossed during the expansion.

There is an overall qualitative agreement between theory and experiments. The CM of the condensate  $|2\rangle$  moves, due to the interaction with the other condensate. The amplitude of the oscillation is in agreement with theory, even though more precise measurements are needed to make the comparison more quantitative. The CM of the condensate  $|1\rangle$  exhibits a damped oscillation. Its frequency is up-shifted compared to the case with no collisions (upper part of the same figure). The measured frequency in the case of colliding condensates is 123.9(3) Hz, with a shift about 6.4(3)%, which is close to the theoretical shift, 5.4%. Furthermore, the oscillations appear now damped with an exponential decay time of about 60 ms. Our theoretical prediction for this decay time is about 170 ms. As already said in the previous sections, the predicted damping originates from inelastic processes in which the energy of the CM motion is transferred to other degrees of freedom. The fact that our theory underestimate the decay time is reasonable if one consider that the theoretical curve in Fig. 6 only includes

the radial degrees of freedom (we solve the coupled GP equations in the  $xy$ -plane). The remaining contribution to the damping can naturally arise from the excitations of axial modes, which are ignored in the present analysis, namely, the possible distortions of the shape of the two condensates along  $z$ , during each collision. A source of damping can also be the occurrence of elastic scattering processes between atoms of the two overlapping condensates, as the one discussed in [20]. These processes are not included in the GP mean-field theory.

In order to compare theory and experiments for the measured aspect ratio, one has to include the effect of the mean-field interaction in the expansion. For the condensate  $|2\rangle$  one can safely use the TF approximation. In practice, one has to solve the coupled equations (11) for the scaling parameters  $b_{\perp}$  and  $b_z$ , after dropping the term linear in  $b$ , which represents the trapping potential. The initial conditions for  $b(0)$  and  $\dot{b}(0)$  are fixed by the configurations of the condensate  $|2\rangle$  in the trap at a given time  $t$ , as calculated in Section IV (see Fig. 5). In Fig. 7 we plot our results, as a function of  $t$ , compared with the experimental data. The oscillations are rather complex, as a result of the periodic collisions between the condensate. The average amplitude is in agreement with the observed data. The slow axial modulation is visible and the faster radial motion has sudden changes of amplitude. Considering that in this comparison there are no fitting parameters, and the theory contains some important approximations, the overall agreement is good, and provides a further evidence of the mutual interaction between the two colliding condensates.

Finally, let us comment on the aspect ratio of the condensate  $|1\rangle$ . This quantity is expected to follow an even more complex evolution, due to the fact that the initial configuration is very far from equilibrium: the trap frequencies are changed by a  $\sqrt{2}$  factor, the condensate is initially displaced from the minimum of its trap and has a shape originally build for  $N$  atoms instead of  $N_1$ . In the TF limit these reduction of the trapping frequencies and of the number of atoms would be equivalent to an “effective” sudden change of the trapping frequencies, of about 96%, if  $N$  were kept fixed. Therefore, due to the non-linearity of the GP equation, the resulting evolution might be chaotic, as predicted in Ref. [21]. Even though the TF approximation is rather poor for this condensate, which has about 20000 atoms, we solved the TF equations for the evolution of  $R_{\perp}/Z$  finding rather irregular oscillations between the extreme values 1 ÷ 15. The comparison with experimental data is thus difficult, even because aspect ratios greater than about 5 are not easy to be measured with the finite resolution of the imaging devices of Ref. [1]. In view of the characterization of the nonlinear (possibly chaotic) dynamics of these condensates, we think that a deeper quantitative analysis of this problem is worth doing in the next future by solving the GP equation in full 3D.

## ACKNOWLEDGMENTS

The authors acknowledge useful discussions with M. Inguscio and S.Stringari. F.D. would like to thank the Dipartimento di Fisica dell'Università di Trento for the hospitality.

## APPENDIX A: SOLVING THE TIME-DEPENDENT GP EQUATION

The GP equations in Eq. (1) can be conveniently rewritten in terms of dimensionless quantities, by rescaling all time and space variables by  $\omega_{\perp} \equiv \omega_{\perp 2}$  and  $a_{\perp} \equiv \sqrt{\hbar/m\omega_{\perp}}$  respectively. In fact, by defining

$$\xi_1 \equiv x/a_{\perp}; \quad \xi_2 \equiv y/a_{\perp}; \quad \xi_3 \equiv z/a_{\perp} \quad (\text{A1})$$

$$\tau \equiv \omega_{\perp} t/2; \quad \psi_i \equiv \sqrt{\frac{a_{\perp}^3}{N}} \Psi_i; \quad u_{ij} \equiv 8\pi N_j a_{ij}/a_{\perp} \quad (\text{A2})$$

we can write Eq. (1) as follows

$$i \frac{\partial \psi_i(\boldsymbol{\xi}, \tau)}{\partial \tau} = \left[ -\nabla_{\boldsymbol{\xi}}^2 + V_i + \sum_{j=1,2} u_{ij} |\psi_j|^2 \right] \psi_i(\boldsymbol{\xi}, \tau) \quad (\text{A3})$$

where the magnetic trapping potential are given by ( $\lambda \equiv \omega_{z2}/\omega_{\perp 2}$ )

$$V_1(\boldsymbol{\xi}) = \frac{1}{2} [\xi_1^2 + (\xi_2 + \xi_{20})^2 + \lambda^2 \xi_3^2] \quad (\text{A4})$$

$$V_2(\boldsymbol{\xi}) = \xi_1^2 + \xi_2^2 + \lambda^2 \xi_3^2, \quad (\text{A5})$$

and the wave functions  $\psi_i$  satisfy the normalization condition ( $i = 1, 2$ )

$$\int d^3 \xi |\psi_i(\boldsymbol{\xi})|^2 = 1. \quad (\text{A6})$$

One of the scheme we use (see Section II) consists in reducing the dynamics to the  $xy$ -plane, by neglecting the axial motion. This corresponds to solve the dynamics of the trapped oscillations in the limit  $\lambda = 0$ , i.e., assuming a uniform wave function along the axial direction. We write  $\psi \equiv A\phi(\xi_1, \xi_2)$ , and we fix  $A$  in order to preserve the width of the condensate profile in the radial direction, when passing from 3 to 2 dimensions (in the TF limit):

$$A = \frac{(15\lambda)^{2/5}}{4} \left( \frac{Na_{22}}{a_{\perp}} \right)^{-1/10}. \quad (\text{A7})$$

Then the GP equations (A3) become

$$\begin{cases} i \frac{\partial \phi_1}{\partial \tau} = \left[ -\nabla^2 + \frac{1}{2} (\xi_1^2 + \xi_2^2) + A^2 \sum_{j=1,2} u_{1j} |\phi_j|^2 \right] \phi_1 \\ i \frac{\partial \phi_2}{\partial \tau} = \left[ -\nabla^2 + \xi_1^2 + (\xi_2 - \xi_{20})^2 + A^2 \sum_{j=1,2} u_{2j} |\phi_j|^2 \right] \phi_2 \end{cases} \quad (\text{A8})$$

and we solve them by using the Split-Step Fourier method [11], with a Fast Fourier Transform algorithm [12], and with the normalization condition ( $i = 1, 2$ )

$$\int d^2 \xi |\phi_i(\boldsymbol{\xi})|^2 = 1. \quad (\text{A9})$$

- 
- \* Dipartimento di Fisica, Università di Padova, via F. Marzolo 8, I-35131 Padova, Italy.
- [1] P. Maddaloni, M. Modugno, C. Fort, F. Minardi and M. Inguscio, cond-mat/0003402.
- [2] C. J. Myatt, E. A. Burt, W. Ghirst, E. A. Cornell and C. E. Wieman, Phys. Rev. Lett. **78**, 586 (1997).
- [3] D. S. Hall, M. R. Matthews, J. R. Ensher, C. E. Wieman, E. A. Cornell, Phys. Rev. Lett. **81**, 1539 (1998).
- [4] D. S. Hall, M. R. Matthews, C. E. Wieman, and E. A. Cornell, Phys. Rev. Lett. **81**, 1543 (1998).
- [5] E. A. Cornell, D. S. Hall, M. R. Matthews, and C. E. Wieman, cond-mat/9808105.
- [6] J. L. Martin, C. R. McKenzie, N. R. Thomas, J. C. Sharpe, D. M. Warrington, P. J. Manson, W. J. Sandle, and A. C. Wilson, J. Phys. B **32**, 3065 (1999).
- [7] J. Williams, R. Walser, J. Cooper, E. A. Cornell, and M. Holland, Phys. Rev. A **61**, 033612 (2000).
- [8] A. Sinatra, P. O. Fedichev, Y. Castin, J. Dalibard, G. V. Shlyapnikov, Phys. Rev. Lett. **82**, 251 (1998).
- [9] A. Sinatra and Y. Castin, Eur. Phys. J. D **8**, 319 (2000).
- [10] F. Dalfovo and M. Modugno, Phys. Rev. A **61**, 023605 (2000).
- [11] B. Jackson, J. F. McCann, and C. S. Adams, J. Phys. B: At. Mol. Opt. Phys. **31**, 4489 (1998).
- [12] W. H. Press *et al.*, *Numerical Recipes* (Cambridge University Press, N.Y. 1986).
- [13] Y. Castin and R. Dum, Phys. Rev. Lett. **77**, 5315 (1996).
- [14] F. Dalfovo, S. Giorgini, L. P. Pitaevskii and S. Stringari, Rev. Mod. Phys. **71**, 463 (1999).
- [15] F. Dalfovo and S. Stringari, Phys. Rev. A **53**, 2477 (1996).
- [16] M. R. Matthews, D. S. Hall, D. S. Jin, J. R. Ensher, C. E. Wieman, and E. A. Cornell, F. Dalfovo, C. Minniti, and S. Stringari, Phys. Rev. Lett. **81**, 243 (1998).
- [17] S. Stringari, Phys. Rev. Lett. **77**, 2360 (1996).
- [18] M. -O. Mewes, M. R. Andrews, N. J. van Druten, D. M. Kurn, D. S. Durfee, C. G. Townsend, and W. Ketterle, Phys. Rev. Lett. **77**, 988 (1996).

- [19] This shift, which arises from the fact that the TF approximation does not include the outer tail of the density at the classical turning point, has to be considered in comparing theory and experiment, since most of the experimental data, as the ones in [1], are extracted by fitting the density distribution with a TF parabola. For this reason, in Fig. 7 we renormalize the initial aspect ratio given by the GP equation to the TF value for the same condensate. This normalization, however, does not affect the main conclusions of our analysis.
- [20] Y. B. Band, M. Trippenbach, J. P. Burke Jr., P. S. Julienne, Phys. Rev. Lett, **84**, 5462 (2000).
- [21] Yu. Kagan, E.L. Surkov and G.V. Shlyapnikov, Phys. Rev. A **55**, R18 (1997).

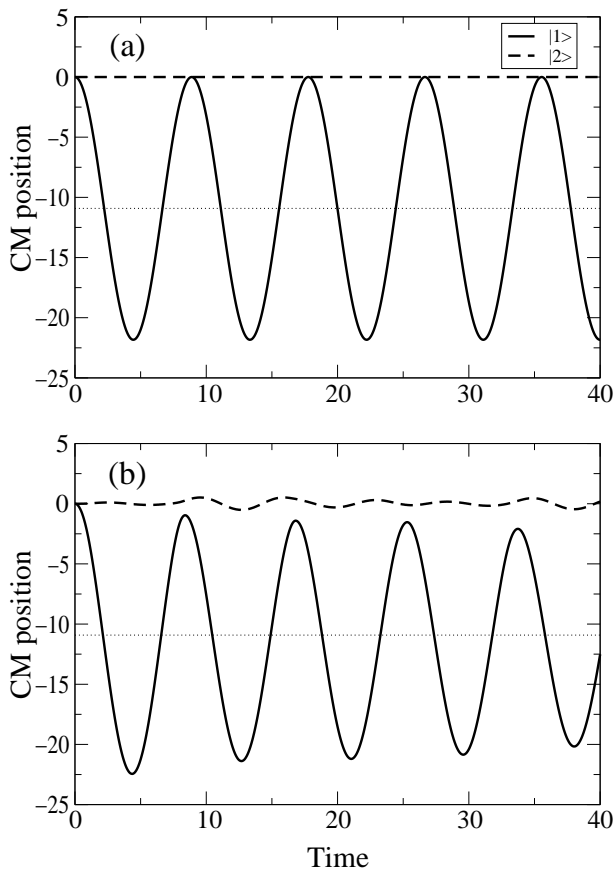


FIG. 1. Center-of-mass oscillations of the  $|1\rangle$  (solid line) and  $|2\rangle$  (dashed line) condensates in the trap: (a) ignoring the mutual interaction, (b) including the mutual interaction. The dotted line corresponds to the equilibrium position  $y = -y_0$  of the  $|1\rangle$  condensate. Time and lengths are given in units of  $\omega_{\perp 2}^{-1}$  and  $a_{\perp 2} = [\hbar/(m\omega_{\perp 2})]^{1/2}$ , respectively.

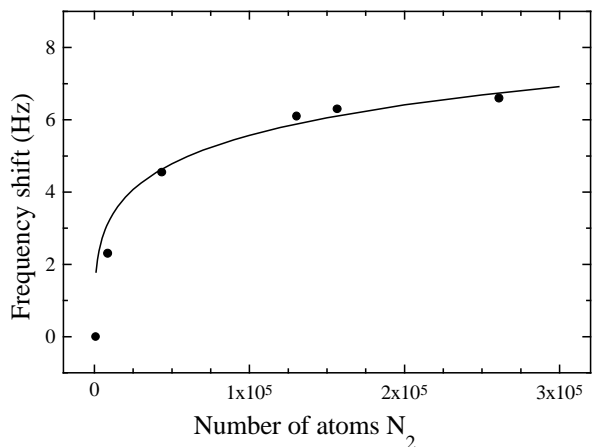


FIG. 2. Frequency shift of the center-of-mass oscillation of the  $|1\rangle$  condensate as a function of the number of atoms  $N_2$  remaining in  $|2\rangle$ . GP results (points) are compared with the classical prediction of Eq. (6) (solid line).

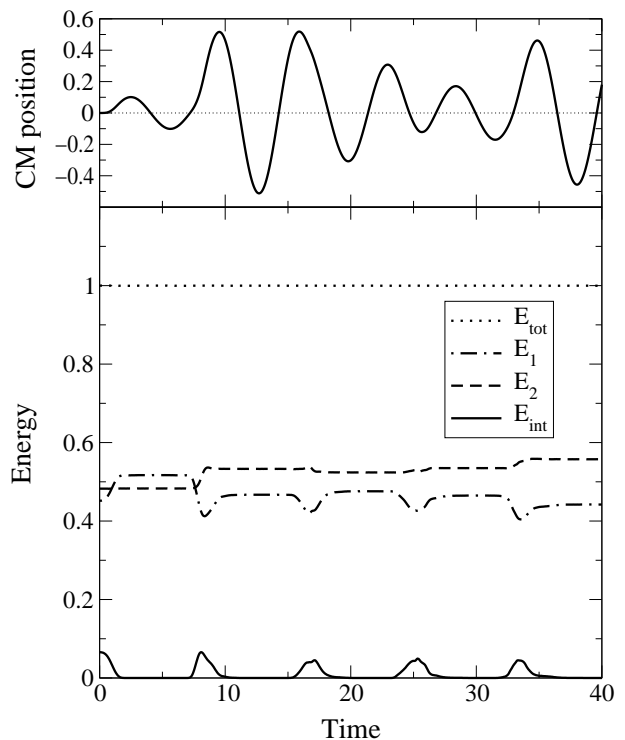


FIG. 3. Plot of the center-of-mass oscillation of  $|2\rangle$  condensate (top) and of the various energy terms contributing to the total energy of the system (bottom), vs. time. The total energy (dotted line) is divided as follows: energy of the  $|2\rangle$  condensate (kinetic + potential + mean-field, dashed), energy of the  $|1\rangle$  condensate (dot-dashed), and interaction energy between the two condensates (solid line).

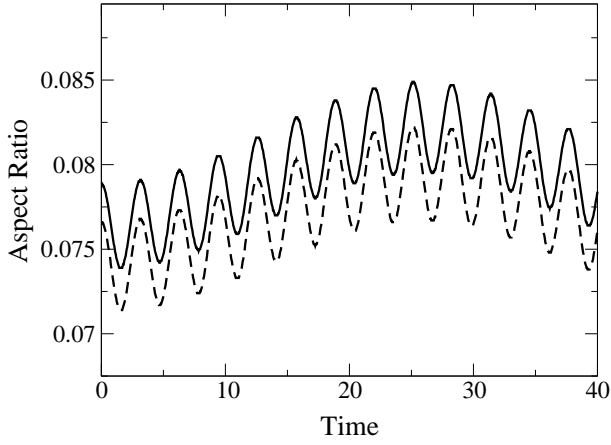


FIG. 4. Evolution of aspect ratio for the  $|2\rangle$  condensate in the trap, as a function of time (in units of  $\omega_{\perp 2}^{-1}$ ) when the interaction with the  $|1\rangle$  condensate is neglected. The solid line is the GP prediction for  $[\langle y^2 \rangle / \langle z^2 \rangle]^{1/2}$ , while the dashed line is  $R_{\perp} / Z$  in the Thomas-Fermi limit.

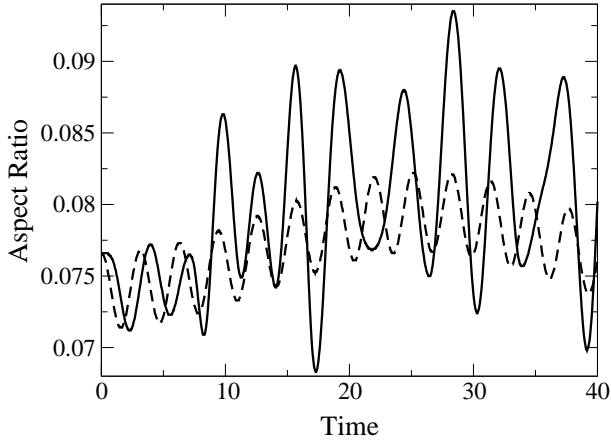


FIG. 5. Evolution of aspect ratio for the  $|2\rangle$  condensate in the trap, as a function of time (in units of  $\omega_{\perp 2}^{-1}$ ). The periodic interaction with the  $|1\rangle$  condensate is included in the case of the solid line and neglected for the dashed line.

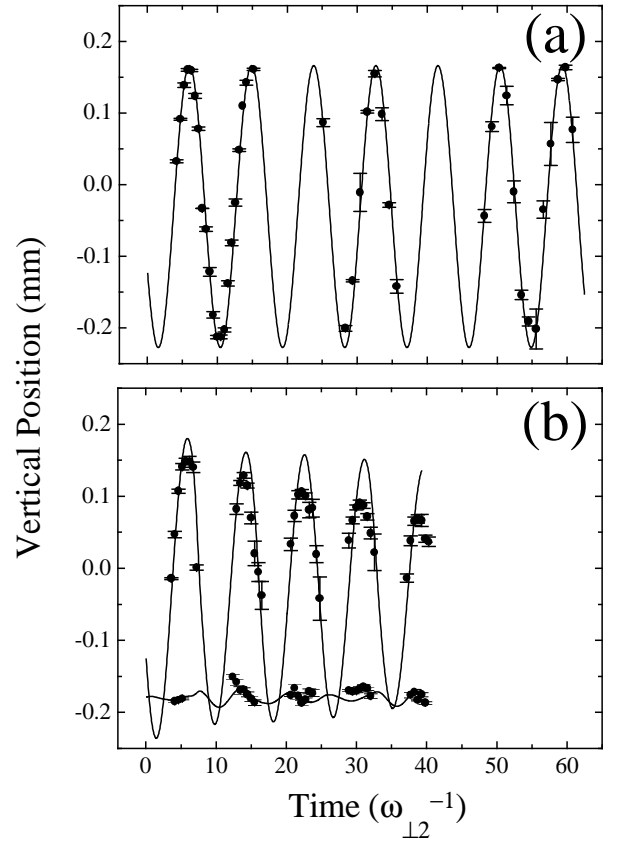


FIG. 6. Center-of-mass oscillations as a function of the trapped evolution time (in units of  $\omega_{\perp 2}^{-1}$ ), after  $t_{exp} = 29.3$  ms of ballistic expansion: a) CM oscillations of the  $|1\rangle$  condensate alone; b) CM oscillations of both condensates, subject to mutual interaction. Theory (solid lines) is compared with experiments (points).

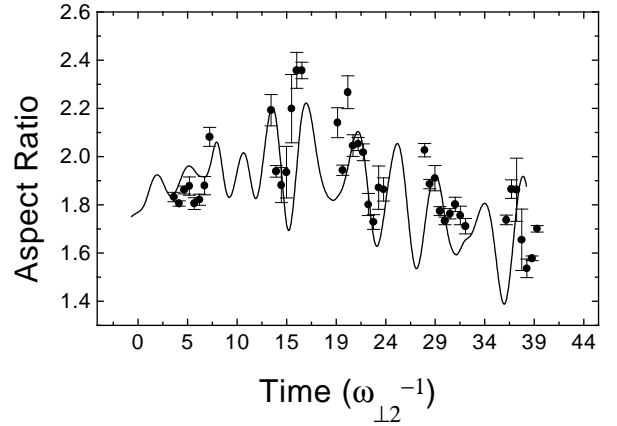


FIG. 7. Aspect ratio for the  $|2\rangle$  condensate, as a function of the trapped evolution time (in units of  $\omega_{\perp 2}^{-1}$ ), after  $t_{exp} = 29.3$  ms of ballistic expansion. The experimental points are compared with the theoretical predictions for the case of two interacting condensates.